BJR

Received: 29 June 2015 | Revised: 23 November 2015 | Accepted: 2 December 2015

doi: 10.1259/bjr.20150530

Cite this article as:
Min M, Lee MT, Lin P, Holloway L, Wijesekera D, Gooneratne D, et al. Assessment of serial multi-parametric functional MRI (diffusion-weighted imaging and R_2*) with 18F-FDG-PET in patients with head and neck cancer treated with radiation therapy. *Br J Radiol* 2016; **89**: 20150530.

FULL PAPER

Assessment of serial multi-parametric functional MRI (diffusion-weighted imaging and R_2*) with ^{18}F-FDG-PET in patients with head and neck cancer treated with radiation therapy

[1,2,3]MYO MIN, FRANZCR, [1,2]MARK T LEE, FRANZCR, MSc, [2,4,5]PETER LIN, FRACP, [1,2,3]LOIS HOLLOWAY, PhD, [3,5]DJ WIJESEKERA, BSc(honours), [2,6]DINESH GOONERATNE, FRANZCR, [1]ROBBA RAI, MHlthSc(MRI), [3]WEI XUAN, PhD, [1]ALLAN FOWLER, FRANZCR, [1,2,3]DION FORSTNER, FRANZCR and [1,2,3,7]GARY LINEY, PhD

[1]Department of Radiation Oncology, Cancer Therapy Centre, Liverpool Hospital, Liverpool, NSW, Australia
[2]South Western Clinical School, School of Medicine, University of New South Wales, NSW, Australia
[3]Ingham Institute of Applied Medical Research, Liverpool, NSW, Australia
[4]Department of Nuclear Medicine and PET, Liverpool Hospital, Liverpool, NSW, Australia
[5]School of Science and Health, Western Sydney University, NSW, Australia
[6]Department of Radiology, Liverpool Hospital, Liverpool, NSW, Australia
[7]Centre for Medical Radiation Physics, University of Wollongong, NSW, Australia

Address correspondence to: Dr Myo Min
E-mail: *Myo.Min@sswahs.nsw.gov.au*.

The authors Allan Fowler and Dion Forstner contributed equally to this work.

Objective: To evaluate the serial changes and correlations between readout-segmented technique with navigated phase correction diffusion-weighted MRI (DWI), R_2*-MRI and ^{18}F-FDG positron emission tomography (PET) CT performed before and during radiation therapy (RT) in patients with mucosal primary head and neck cancer.

Methods: The mean apparent diffusion coefficient (ADC_{mean}) from DWI (at $b = 50$ and 800 s mm^{-2}), the mean R_2* values derived from T_2*-MRI, and PET metabolic parameters, including maximum standardized uptake value (SUV_{max}), metabolic tumour volume (MTV) and total lesional glycolysis (TLG) were measured for the primary tumour. Spearman correlation coefficients were calculated to evaluate correlations between ADC_{mean}, R_2*, SUV_{max}, MTV and TLG. A paired *t*-test was performed to assess the MRI changes and the slope of serial MRI changes during RT.

Results: Pre-treatment scans were performed in 28 patients and mid-treatment scans in 20 patients. No significant correlation was found between ADC_{mean} and either R_2* values or PET parameters. There were significant negative correlations of R_2* values with pre-treatment PET parameters but not with mid-RT PET parameters: pre-SUV_{max} ($p = 0.008$), pre-MTV ($p = 0.006$) and pre-TLG ($p = 0.008$). A significant rise in ADC_{mean} was found during the first half ($p < 0.001$) of RT but not in the second half ($p = 0.215$) of the treatment. There was an increase of the ADC_{mean} values of 279.4 [95% confidence interval (95% CI): 210–348] in the first half of the treatment (Weeks 0–3). However, during the second-half period of treatment, the mean ADC value (Weeks 3–6) was 24.0 and the 95% CI (−40 to 88) included zero. This suggests that there was no significant change in ADC values during the second half of the treatment.

Conclusion: A significant negative correlation was found between pre-treatment R_2*-MRI and PET parameters. DWI appeared to demonstrate potentially predictable changes during RT.

Advances in knowledge: Understanding the correlation and changes that occur with time between potential imaging biomarkers may help us establish the most appropriate biomarkers to consider in future research.

INTRODUCTION

In order to individualize and optimize the treatments for patients with mucosal primary head and neck cancer (MPHNC) treated with radiation therapy (RT), prognostic and predictive biomarkers are required, either before or during treatment to allow effective early intensification or de-escalation of treatments. Imaging biomarkers with fluorine-18 fludeoxyglucose positron emission tomography (^{18}F-FDG-PET) or MRI have the benefit of being non-invasive, reproducible and repeatable allowing serial measurements to be performed during treatment.

^{18}F-FDG-PET has an established role in head and neck cancer (HNC) management including staging and RT response assessment, and also in adaptive RT.[1–3] Since maximum standardized uptake value (SUV_{max}) is the most commonly used parameter in diagnostic or staging ^{18}F-FDG-PET, several studies have reported its prognostic significance especially performed before RT.[1] Recently, the predictive value of novel parameters such as metabolic tumour volumes (MTVs) and total lesional glycolysis (TLG) has been investigated before and during treatment and found to correlate with patient outcome.[1,4,5]

Diffusion-weighted MRI (DWI), a non-contrast imaging study, can evaluate the motion of water in a specified region of interest (ROI) by means of the apparent diffusion coefficient (ADC) which reflects the distribution of water molecules within the tumour.[6] Some recent studies have also shown its role in therapeutic response prediction before and during RT.[7,8] High magnetic field strength such as 3.0 T can improve the signal-to-noise ratio but can result in increased distortion for DWI undertaken using single-shot echo planar imaging (EPI). The readout-segmented technique with navigated phase correction for DWI has been shown to reduce distortion in other tumour sites.[9–11] We have previously shown that this implementation of DWI results in similar geometrically shaped anatomical imaging in the prostate,[12] making it more feasible to correlate with other imaging sequences and/or modalities. However, it has not been evaluated in HNC.

Hypoxia is known to be associated with treatment failures in several tumour sites.[13] Changes in blood oxygenation levels can be evaluated indirectly by measurements such as R_2* which can increase owing to modulating magnetic field gradients around blood vessels as the fraction of oxyhaemoglobin to deoxyhaemoglobin reduces.[14,15] Although an animal study showed no correlation between R_2* changes and absolute pO_2,[16] Chopra et al[17] reported a significant correlation between R_2* and hypoxia measured by the Eppendorf electrode in prostate cancer and Li et al[18] reported the predictive role of R_2* in advanced cervical squamous cell carcinoma. However, use of R_2* in HNC remains investigational, as no published study has assessed the role of R_2* in HNC and further evaluation is required to determine its potential use.

To our knowledge, the correlation between R_2*, ADC and ^{18}F-FDG-PET for HNC has not been considered previously. The aim of this study was to investigate the potential role of these non-contrast MRI measurements and assess any correlations with ^{18}F-FDG-PET performed before and during RT in patients with MPHNC. Serial changes of both DWI and R_2* were also evaluated in this study to assess possible patterns of MRI changes during RT that may be helpful in determining the optimal timing of imaging performed during radiotherapy to assess response.

METHODS AND MATERIALS

Patients

After receiving local research ethics committee approval, patients with newly diagnosed, biopsy-proven, non-metastatic MPHNC, suitable for radical RT with or without chemotherapy were recruited for this prospective study from May 2014 to February 2015. Written informed consent was obtained from every patient included in this study. At our institution, patients routinely receive ^{18}F-FDG-PET before and at the third week of RT. The study timeline is shown in Figure 1. The primary end point of the study were the changes in multiparametric MRI (DWI and R_2*) before and during RT at different time points against locoregional failure-free survival. The recruitment has been completed for the study, but the oncological outcome data are awaited. An interim analysis of images was performed in order to evaluate the correlations between different imaging parameters.

MRI acquisition and image analysis

MRI was performed on a dedicated wide-bore 3.0-T scanner (MAGNETOM® Skyra; Siemens Healthcare, Erlangen, Germany) before and during RT (second, third, fifth and sixth weeks). Sequences obtained were DWI acquired, using a readout-segmented EPI

Figure 1. A flow chart illustrating the study time line. The blue box indicates standard imaging studies; the green box indicates investigational studies. ^{18}F-FDG-PET, fluorine-18 fludeoxyglucose positron emission tomography; DWI, diffusion weighted MRI; RT, radiation therapy. For colour images see online.

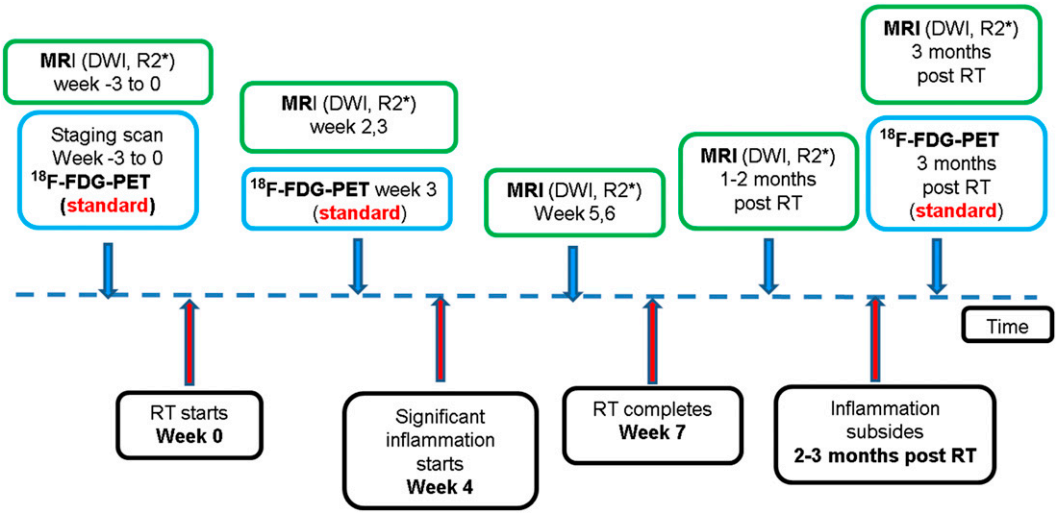

technique (RESOLVE; Siemens Healthcare), using $b = 50$ and 800 s mm^{-2} with signal averages set to 1 and 3, respectively. A multiple gradient echo sequence was used for the calculation of R_2* using eight echoes (echo time = 5, 15, 25, 34, 44, 54, 64 and 74 ms) and repetition time = 500 ms. Pixel-by-pixel maps of ADC and R_2* were calculated using the scanner console and off-line Fiji software[19] (using the MRI processor plug-in), respectively.

The initial five patients were scanned using two four-channel surface coils placed over the thermoplastic mask in the RT treatment positions. This was initially chosen because a longer term study aim is to investigate the feasibility of adaptive RT. However, owing to intolerance by patients, later scans were performed using a dedicated 16-channel head and neck coil. The quality of the MRI images was reviewed by a MRI physicist, radiation oncologist and radiologist to determine suitability for subsequent analysis.

Tumour ROIs were drawn on axial images of ADC maps or R_2* maps with reference to T_2 weighted images by the same radiologist, radiation oncologist and MRI physicist. We adopted the method described by Li et al,[18] and a total of three ROIs (for each patient) were contoured and the areas of the largest dimension were chosen wherever possible. The mean values of R_2* or ADC were then calculated from the three ROIs.

^{18}F-FDG-PET-CT acquisition and metabolic parameter measurement

The studies were acquired in RT treatment position on a GE Discovery™-710 time-of-flight positron emission tomography (PET)-CT (GE Healthcare, Waukesha, MI). Patients received 4.1 MBq kg^{-1} of ^{18}F-FDG after at least 4 h of fasting. Details of the imaging technique, ^{18}F-FDG-PET-CT image interpretation, metabolic parameters measurements and segmentation methodology have been described in our previous study reporting the predictive role of interim PET (mid-treatment) for HNC.[5] Although PET images were reviewed independently from MRI images, in order to get consistent ROIs, the same radiation oncologist who analysed the MRI images was present for all PET imaging reviews and analyses.

Statistical analysis

Spearman correlation was performed to evaluate the correlation between imaging parameters: pre-treatment and mid-treatment ^{18}F-FDG-PET metabolic parameters *vs* ADC values *vs* R_2* values; serial changes in mean ADC values *vs* R_2* values. A paired *t*-test was performed to assess if any significant MRI changes occurred at different time points during RT. For every individual patient, two separate least square lines were fitted. The first line was based on measurements at Weeks 0, 2 and 3, which provided the estimate of the slope of the line for the first half of the treatment duration. The second least square line for every individual was fitted using the measurements at Weeks 3, 5 and 6, which provided the estimate of the slope of the line for the second half of the treatment duration. Mean values of slopes for the first and second halves were presented with a 95% confidence interval (95% CI) and also compared using a paired *t*-test. Statistical analysis was performed using the IBM SPSS® Statistics v. 22.0

Table 1. Patients/tumour characteristics and treatment summary

Characteristics	
Total	28
Age (years)	
Median	61
Range	49–80
Sex	
Male	25 (89.3%)
Female	3 (10.7%)
Primary tumour site	
Oropharynx (total)	17 (60.7%)
p16 positive	5
p16 negative	1
p16 unknown (*e.g.* insufficient specimens)	11
Larynx	7 (25.0%)
Nasopharynx	4 (14.3%)
T stage	
1	2 (7.1%)
2	14 (50.0%)
3	8 (28.6%)
4	4 (14.3%)
N stage	
0	6 (21.4%)
1	2 (7.1%)
2 (total)	18 (64.3%)
2 (NPC)	1 (3.6%)
2a (non-NPC)	0 (0%)
2b (non-NPC)	11 (39.3%)
2c (non-NPC)	6 (21.4%)
3	2 (7.1%)
Staging (overall)	
II	5 (17.9%)
III	5 (17.9%)
IV	18 (64.3%)
Treatment	
Radiotherapy only	4 (14.3%)
Chemoradiotherapy (weekly cisplatin)	19 (67.6%)
Radiotherapy + cetuximab	3 (10.7%)
Induction chemotherapy followed by chemoradiotherapy (weekly cisplatin)	1 (3.6%)
Primary surgery	1 (3.6%)

NPC, nasopharyngeal cancer.

(IBM Corporation, Armonk, NY; formerly SPSS Inc. Chicago, IL) and Microsoft® Excel® 2010 (Microsoft, Redmond, WA). Statistical significance was considered at the $p = 0.05$ level.

RESULTS

28 eligible patients were enrolled in this prospective feasibility study during May 2014 to February 2015. Primary tumour sites were oropharynx ($n = 17$), larynx ($n = 7$) and nasopharynx ($n = 4$). Median age was 61 years (range 49–80 years), male : female ratio was 25 : 3 and staging was based on the American Joint Committee on Cancer 7th Edition comprised of 4 patients in Stage II, 5 in Stage III and 19 in Stage IV. Details of patient characteristics and treatment details are summarized in Table 1.

All patients were treated with intensity-modulated radiotherapy or helical TomoTherapy® (Accuray, Sunnyvale, CA): the total dose to the gross tumour volume (primary tumour or bulky lymph nodes of ≥1 cm) was 60–70 Gy; high-risk cervical lymph node regions received 60–66 Gy; and the low risk regions received 56 Gy. As shown in Table 1, the majority of patients received concurrent chemotherapy using weekly cisplatin ($40\ mg\ m^{-2}$) while four patients were treated with RT only, three with concurrent weekly cetuximab ($250\ mg\ m^{-2}$) and one with induction chemotherapy (two cycles of three weekly cisplatin $80\ mg\ m^{-2}$ and etoposide $113\ mg\ m^{-2}$) followed by concurrent weekly cisplatin ($40\ mg\ m^{-2}$).

All 28 patients received pre-treatment scans, and 20 patients received mid-treatment scans. Six patients withdrew from the study for several reasons including anxiety, claustrophobia and "too many appointments". One patient decided to have primary surgery instead of primary RT, and another patient decided not to have any treatment owing to personal/social reasons. Of the remaining 20 patients who received mid-treatment scans, 3 patients did not have all mid-treatment scans, leaving 17 patients who had all 4 scans during radiotherapy: 1 patient missed 2 scans and 2 patients missed 1. Therefore, 20 patients were included in further analysis of correlation between different images, but only 17 patients were included for the analysis of serial changes.

Serial changes in ADC, R_2* and ^{18}F-FDG-PET metabolic parameters were observed and summarized in Table 2. As shown in Table 3, pre-treatment ^{18}F-FDG-PET metabolic parameters were found to be negatively correlated with R_2* values, but the results were not statistically significant for mid-treatment parameters. However, there was no significant correlation seen between mean ADC (ADC_{mean}) values and either R_2* values or any of the ^{18}F-FDG-PET metabolic parameters (Table 3). Figure 2 demonstrates the correlation between SUV_{max} and R_2* before and during RT by means of Scatter plots. In addition, there was no association between minimum ADC or maximum ADC and SUV_{max} values (detailed data not shown).

The changes which occurred in any of the functional imaging parameters ($\Delta SUV_{max}/\Delta MTV/\Delta TLG$, ΔR_2* and ΔADC) at the third week of RT showed no correlation between each other (Table 4). In addition, there was no correlation between

Table 2. Summary of mean apparent diffusion coefficient (ADC_{mean}), mean R_2* (R_2*$_{mean}$) and fluorine-18 fludeoxyglucose positron emission tomography metabolic parameters

Parameters	Median	Range
Pre-treatment		
SUV_{max} ($g\ ml^{-1}$)	12.1	3.7–22.0
MTV (cm^3)	21.5	1.0–122
TLG (g)	92.9	2.7–924
ADC_{mean} ($\times 10^{-3}\ mm^2\ s^{-1}$)	1.177	0.808–1.678
R_2*$_{mean}$ (s^{-1})	0.0600	0.0341–0.1175
Week 2		
ADC_{mean} ($\times 10^{-3}\ mm^2\ s^{-1}$)	1.553	1.112–2.100
R_2*$_{mean}$ (s^{-1})	0.0557	0.0283–0.089
Week 3		
SUV_{max} ($g\ ml^{-1}$)	8.1	2.4–15.1
MTV (cm^3)	7.15	0.0–43.3
TLG (g)	27.95	0.0–241.2
ADC_{mean} ($\times 10^{-3}\ mm^2\ s^{-1}$)	1.724	1.037–2.510
R_2*$_{mean}$ (s^{-1})	0.0595	0.0393–0.1195
Week 5		
ADC_{mean} ($\times 10^{-3}\ mm^2\ s^{-1}$)	1.653	1.170–2.501
R_2*$_{mean}$ (s^{-1})	0.0632	0.0435–0.1158
Week 6		
ADC_{mean} ($\times 10^{-3}\ mm^2\ s^{-1}$)	1.738	0.919–2.190
R_2*$_{mean}$ (s^{-1})	0.0589	0.0401–0.1011

MTV, metabolic tumour volume; SUV_{max}, maximum standardized uptake value; TLG, total lesional glycolysis.

ΔADC_{mean} and ΔR_2*$_{mean}$ at any time point (Week 2, 3, 5 or 6) during RT. The box plots of serial ADC and R_2* changes during RT are shown in Figure 3.

As shown in Figure 4a, it appears that there is a significant rise in ADC values from pre-RT (Week 0) to Week 2 or 3, but there is a plateau from Weeks 3–6. On paired *t*-test, there was a significant rise in ADC values from Week 0 to either Week 2 ($p < 0.0001$) or Week 3 ($p \leq 0.0001$), but there was no significant increase in ADC values from Weeks 3–5 or Week 6.

There was an increase of the ADC_{mean} values of 279.4 (95% CI: 210–348) in the first half of treatment (Weeks 0–3). However, during the second half period of treatment, the mean ADC value (Weeks 3–6) was 24.0 and the 95% CI (−40 to 88) included zero. This suggests that there was no significant change in ADC values during the second half of treatment.

As shown in Figure 4b, the serial R_2* changes were found to be erratic, and it was not possible to make a meaningful conclusion. A further analysis in correlation with oncological outcomes is required.

Table 3. Summary statistics of correlation between mean apparent diffusion coefficient (ADC_{mean}) values, mean R_2^* ($R_2^*{}_{mean}$) values and fluorine-18 fludeoxyglucose positron emission tomography (^{18}F-FDG-PET) parameters: pre-treatment and mid-treatment (Week 3)

Parameters	Spearman correlation	
	ADC_{mean}	$R_2^*{}_{mean}$
Pre-treatment		
SUV_{max}	−0.264 ($p = 0.193$)	−0.528 ($p = 0.008$)
SUV_{mean}	−0.323 ($p = 0.108$)	−0.498 ($p = 0.013$)
MTV	−0.320 ($p = 0.111$)	−0.546 ($p = 0.006$)
TLG	−0.322 ($p = 0.109$)	−0.525 ($p = 0.008$)
$R_2^*{}_{mean}$	0.225 ($p = 0.301$)	
Week 3		
SUV_{max}	0.076 ($p = 0.763$)	−0.405 ($p = 0.096$)
SUV_{mean}	0.067 ($p = 0.797$)	−0.240 ($p = 0.338$)
MTV	0.108 ($p = 0.669$)	−0.424 ($p = 0.079$)
TLG	−0.005 ($p = 0.984$)	−0.459 ($p = 0.055$)
$R_2^*{}_{mean}$	0.160 ($p = 0.514$)	

MTV, metabolic tumour volume; SUV_{max}, maximum standardized uptake value; SUV_{mean}, mean standardized uptake value; TLG, total lesional glycolysis.

DISCUSSION

This is the first study reporting the correlations between DWI, R_2^*-MRI and ^{18}F-FDG-PET in HNC. Our study is also the first study assessing serial changes of both DWI and R_2^*-MRI during RT in HNC.

To our knowledge, there is no study to date which evaluates the correlation between ADC and R_2^* in any tumour site. Our study shows no correlation between the two parameters, but this is not unexpected because DWI detects tumour cellularity, whereas R_2^* assesses regional oxygenation. At best, they would provide additional independent prognostic information and should be used in conjunction with each other.

R_2^* is a relative measure of oxygenation within a specified ROI. Our study shows that there is a negative correlation between pre-treatment R_2^* with all measures of ^{18}F-FDG-PET metabolic activity (SUV_{max}, TLG and MTV), suggesting aerobic glycolysis is the dominant mechanism driving altered glucose metabolism in MPHNC and limited role of using ^{18}F-FDG uptake as a surrogate marker of hypoxia. Another contributing factor may be due to necrotic areas within hypoxic tumours (with high R_2^* values) having reduced consumption of glucose and resulting in reduced overall metabolic activity (with low ^{18}F-FDG-PET parameter values). Although statistically significant, the degree of correlation was noted to be moderate rather than high (Spearman correlation range 0.498–0.546). This may be due to the presence of outliers such as low R_2^* with low ^{18}F-FDG status (well oxygenated but low metabolic activity and likely to be very good responders) and high R_2^* with high ^{18}F-FDG status (hypoxic but metabolically active tumours and likely to be poor responders). We believe that R_2^* data are likely to add more prognostic information in HNC when treated with RT.

One limitation of R_2^*-MRI is that it is a relative measurement of deoxygenated haemoglobin rather than an absolute oxygenation concentration. Therefore, caution would need to be exercised when interpreting changes, as this method is also very sensitive to changes in blood flow, volume and pH.[14] We believe that R_2^* is likely to be a complementary imaging biomarker to other

Figure 2. Correlation between maximum standardized uptake value (SUV_{max}) and R_2^* (a) before and (b) during radiation therapy (Week 3). CC, correlation coefficient.

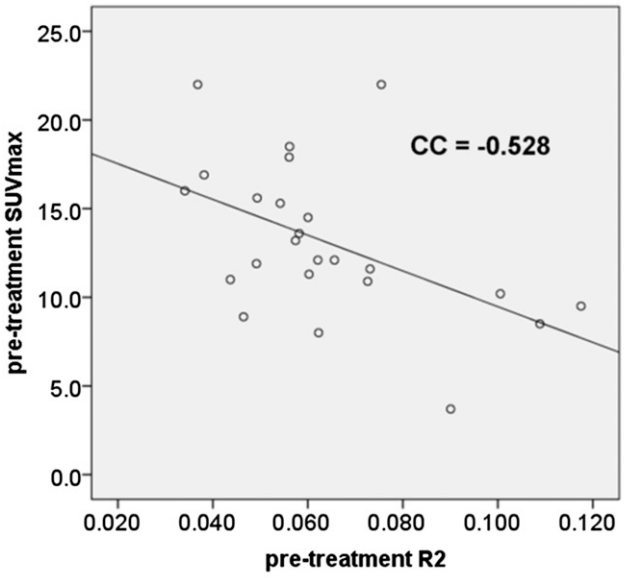

(A)

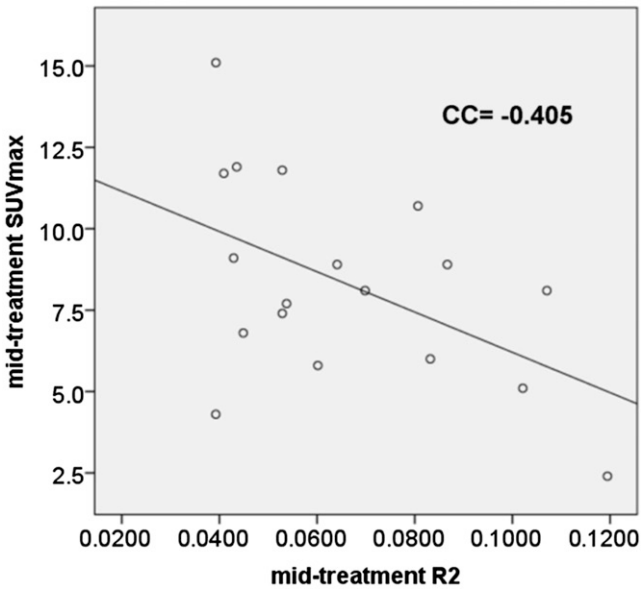

(B)

Table 4. Correlation between changes in mean apparent diffusion coefficient (ADC_{mean}) values, mean R_2^* ($R_2^*{}_{mean}$) values and fluorine-18 fludeoxyglucose (^{18}F-FDG-PET) positron emission tomography at the third week of radiation therapy

Parameters	Spearman correlation	
	ΔADC_{mean}	$\Delta R_2^*{}_{mean}$
ΔSUV_{max}	−0.064 ($p = 0.801$)	−0.053 ($p = 0.845$)
ΔSUV_{mean}	0.239 ($p = 0.341$)	0.097 ($p = 0.720$)
ΔMTV	−0.160 ($p = 0.526$)	0.047 ($p = 0.863$)
ΔTLG	−0.181 ($p = 0.473$)	0.118 ($p = 0.664$)
$\Delta R_2^*{}_{mean}$	0.223 ($p = 0.390$)	

MTV, metabolic tumour volume; SUV_{max}, maximum standardized uptake value; SUV_{mean}, mean standardized uptake value; TLG, total lesional glycolysis.

function imaging studies. Although R_2^* and PET were found to be correlated, it is not known whether R_2^* can improve the sensitivity and specificity of ^{18}F-FDG-PET in prediction of treatment response. Further evaluations should be performed in future to identify the actual hypoxic subvolumes within the ROIs in correlation with treatment outcomes.

Figure 5 shows an example of a patient with left tonsil cancer with significant changes demonstrated in serial multiparametric MRI and ^{18}F-FDG-PET. This case was chosen because the serial changes during RT, in particular R_2^*, were most obvious. However, as shown in Figure 3b, in the majority of cases, serial changes in R_2^* seemed to be either more subtle or erratic. The changes in R_2^* during RT do not seem to demonstrate any pattern. This may be due to the fact that hypoxia or level of oxygenation may be variable at different time points or different locations within the ROI. The level of oxygenation could also be variable because hypoxia may be acute or chronic.[20] Furthermore, it may well be that a correlation between changes in R_2^* before or during RT and oncological outcomes may be visible only on a voxel (subregion) basis. Since the mean values inside the ROIs (the mean over all voxels) were evaluated in this study, these values may not represent the actual hypoxic subvolumes. We believe that further studies correlating R_2^* and other imaging studies, using hypoxia-specific tracers [*e.g.*

Figure 3. Box plots of serial mean apparent diffusion coefficient (ADC) and R_2^* changes during radiation therapy. (a) ADC values and (b) changes in ADC values at different time points (*e.g.* pre-treatment ADC values minus Week 2 ADC values). (c) R_2^* values (d) changes in R_2^*values at different time points (*e.g.* pre-treatment R_2 values minus Week 2 R_2 values).

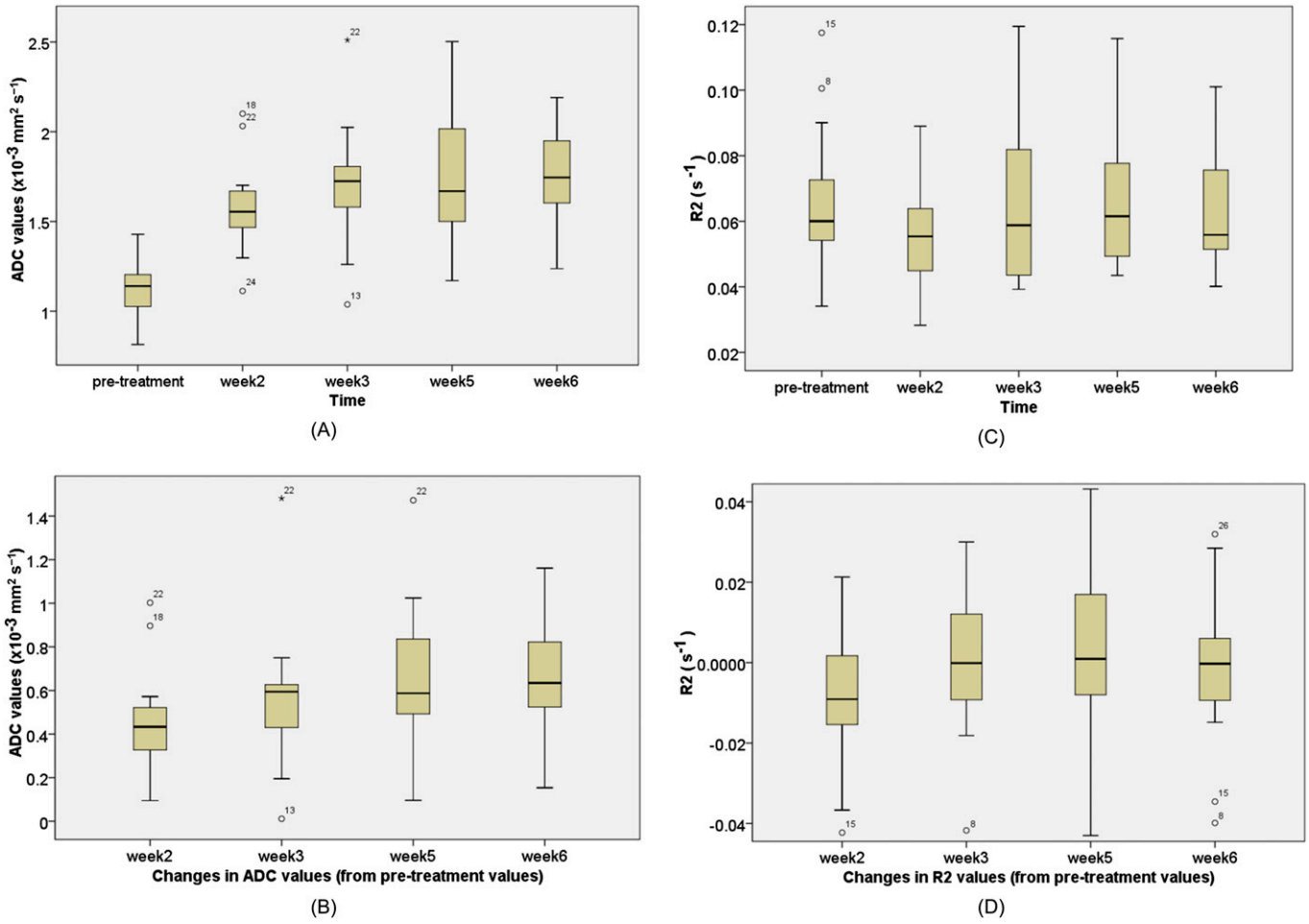

Figure 4. Serial MRI changes during radiation therapy: (a) mean apparent diffusion coefficient (ADC) changes and (b) R_2* changes. *The patient in Figure 5. RT, radiation therapy.

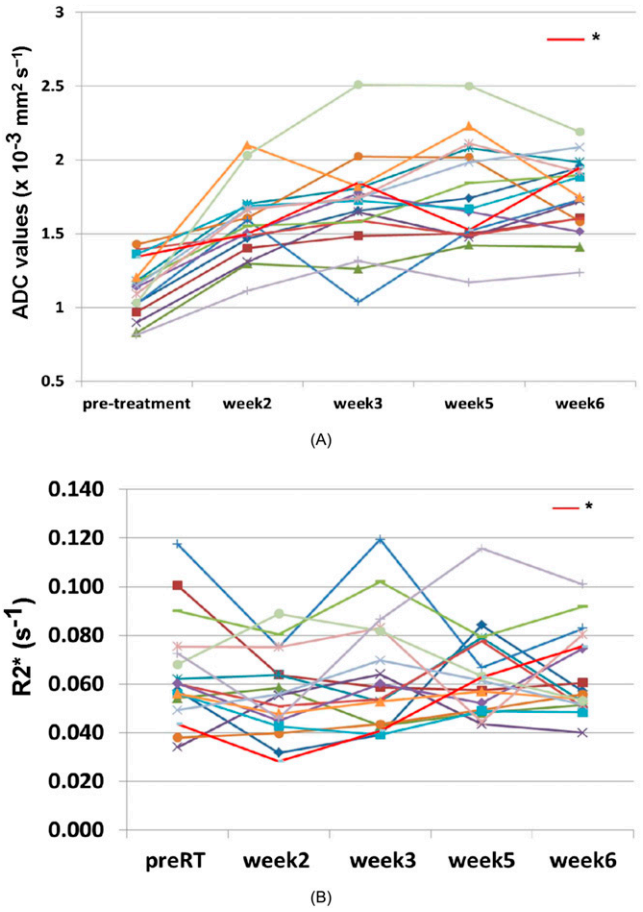

^{18}F-fluoromisonidazole/^{18}F-fluoroazomycin arabinoside (FMIZO/FAZA)] would be useful to confirm the predictive role of this novel MRI sequence and also to help define ROIs that would be most representative of hypoxic subvolumes on R_2* images. Analysis of histogram distributions may also be more revealing than simply using mean value which will mask heterogeneity. Nevertheless, the oncological outcome data are required to make a meaningful conclusion.

Choi et al[21] reported no correlation between ADC_{mean} and SUV_{max} or SUV_{mean} using a 1.5-T MRI scanner and the *b*-values of 1000 and 2000 s mm^{-2}. Using the relatively new readout-segmented technique, a different *b*-value of 800 s mm^{-2} and a higher magnetic field strength scanner (3.0 T), as shown in Table 2, our results were found to be comparable to their results. Our study demonstrated no correlation of ADC values with SUV_{max} or SUV_{mean} and also no correlation with more novel parameters such as MTV or TLG. Since DWI reflects tumour cellularity while ^{18}F-FDG-PET represents tumour metabolic activity, one would generally assume that they are likely to correlate. However, as discussed by Choi et al,[21] owing to tumour heterogeneity, there is no association between ADC values (using either high or low *b*-values) and ^{18}F-FDG parameters.

It is reasonable to hypothesize that changes (or decreases) in cellularity within the tumour during RT would be consistent at different time points, especially if the tumour is responding to therapy. A non-invasive tool is, however, required to evaluate these changes in response to therapy. As shown in Figure 4a, the majority of patients showed a rise in ADC values in the second and third weeks of RT (more significant during the second week) but not in the second half of treatment (Week 3 to either Week 5 or 6). This appearance was confirmed on paired *t*-test where there is a significant change in the first half (Weeks 0–2 or Week 3, $p < 0.001$) but not in the second half (from Weeks 3–5 or Week 6, $p = 0.215$). In addition, the mean slope of the within-patient least square line was significantly above zero for the first half of the treatment duration but not in the second half. These findings suggest that imaging changes as early as Week 2 or 3 may show changes in tumour cellularity, and these changes plateau following that time point.

It is possible that smaller residual tumours, with surrounding oedema and inflammation, may confound the accurate identification of ROIs that represent the actual tumour and effect accurate tumour ADC measurements beyond 3 weeks. Because of this, there may be a significant interobserver variability that could influence the ADC results in the fifth and sixth weeks. Our findings suggest that either Week 2 or 3 is likely to be more reliable in therapeutic response prediction or assessment during treatment. Performing scans in the first half would also allow sufficient time to implement adaptive therapy. However, we are planning to perform a detailed analysis of patterns of changes in cellularity in responders *vs* non-responders to treatment from all time points assessed in this study. The actual optimal timing to identify good or poor responders is still not known and will require further investigation.

Schouten et al[22] reported no correlation between ΔSUV_{mean} or ΔSUV_{max} and ΔADC at the third week of RT in patients with HNC. They compared EPI with half-fourier acquisition single-shot turbo spin-echo DWI using 1.5-T scanner, but none of them showed any correlation with ^{18}F-FDG-PET data. As shown in Table 4, our study also showed no correlation between the DWI, using 3.0 T, and all metabolic parameters of ^{18}F-FDG-PET at the third week. In addition, no correlation between any of the functional parameters (DWI, R_2* and ^{18}F-FDG-PET) suggests that responses shown by each functional imaging study are likely to be independent of each other.

Our study has confirmed that it is feasible to perform multiparametric functional MRI at multiple time points. Patients were found to tolerate the head coils rather than the thermoplastic mask with surface coils, especially during RT. Given that a correlation was found between R_2*-MRI and ^{18}F-FDG-PET but not between either R_2*-MRI or ^{18}F-FDG-PET with DWI, use of multiple imaging biomarkers for prognosis or treatment response is likely required. Further correlation studies such as R_2*-MRI *vs* PET using hypoxic tracers (*e.g.* FMIZO/FAZA) and DWI *vs* PET using proliferation markers (*e.g.* ^{18}F-labelled fluoro-30-deoxy-30-L-fluorothymidine) would be useful to determine whether these MRI scans can be used as alternatives. Limitations of PET scans, including radiation exposure,

Figure 5. Serial MRI and fluorine-18 fludeoxyglucose positron emission tomography images of a patient with left tonsil cancer. ADC, apparent diffusion coefficient maps; PET, positron emission tomography images; R_2*, R_2* weighted images; T2, T_2 weighted images.

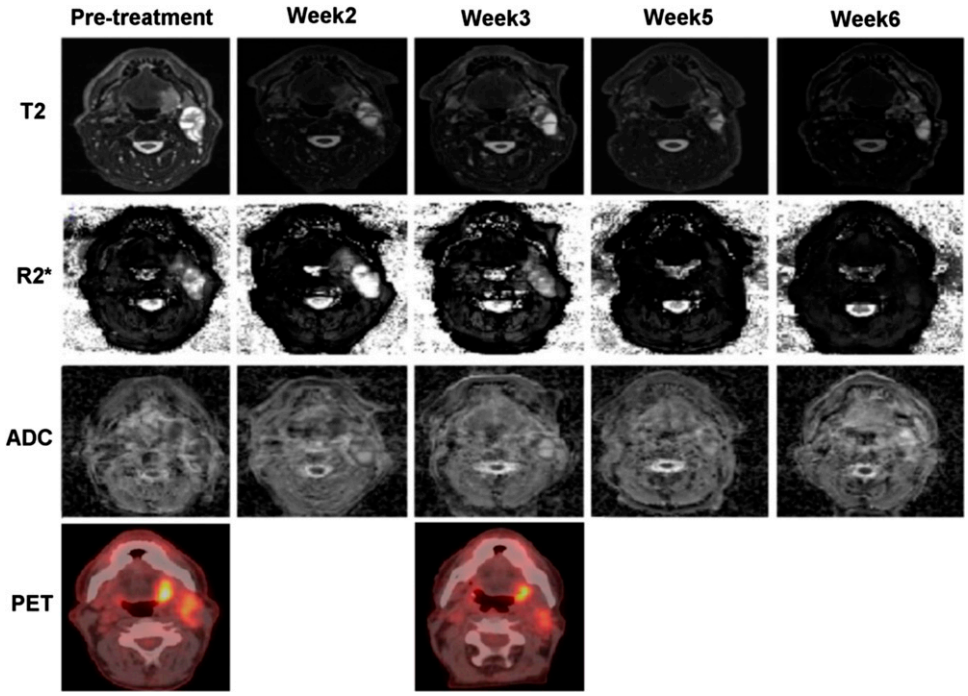

requirement of tracers that are relatively expensive, longer scanning time and low spatial resolution, can be avoided by using MRI scans.

One limitation of the study is that all the MRI parameters (ADC and R_2*) analysed in this study were based on ROIs of residual abnormal diffusion or R_2* changes. It is important to note that ROIs of functional MRI could reduce in size disproportionate to the corresponding anatomical images used as references. This could result in underestimating the changes compared to if the whole anatomical residual tumours were used. Furthermore, all the MRI and PET images were analysed independently with reference to either T_2 weighted images or CT images. Registration may have been improved if scans were undertaken in the same position, ideally using radiotherapy fixation masks and surface coils. However, by using a dedicated head and neck radiofrequency coil, we were able to improve patient compliance and gain valuable signal-to-noise ratio in our functional imaging. This improves image quality and makes identification of ROIs easier. Registration accuracy was not investigated in this study, and although our method aimed at minimizing the error and is consistent with other published studies correlating MRI and ^{18}F-FDG-PET studies in HNC,[21,23] this should be addressed in the future.

CONCLUSION

Our study has shown that pre-treatment R_2*-MRI values were significantly correlated with ^{18}F-FDG-PET parameters. Future investigations into imaging biomarkers for identifying poor or good responders may be improved by a combination of R_2*-MRI and ^{18}F-FDG-PET. Although there is no correlation with either ^{18}F-FDG-PET or R_2*-MRI, DWI appeared to demonstrate potentially predictable changes in response to RT, especially in the first half during treatment, and it may be a useful biomarker in monitoring therapy response. Correlations with oncological outcomes are required to validate our findings.

FUNDING

This study was supported by the RANZCR research grant in 2014.

REFERENCES

1. Paidpally V, Chirindel A, Lam S, Agrawal N, Quon H, Subramaniam RM. FDG-PET/CT imaging biomarkers in head and neck squamous cell carcinoma. *Imaging Med* 2012; **4**: 633–47. doi: 10.2217/iim.12.60
2. Berwouts D, Olteanu LA, Duprez F, Vercauteren T, De Gersem W, De Neve W, et al. Three-phase adaptive dose-painting-by-numbers for head-and-neck cancer: initial results of the phase I clinical trial. *Radiother Oncol* 2013; **107**: 310–16. doi: 10.1016/j.radonc.2013.04.002
3. Olteanu LA, Berwouts D, Madani I, De Gersem W, Vercauteren T, Duprez F, et al. Comparative dosimetry of three-phase adaptive and non-adaptive dose-painting IMRT for head-and-neck cancer. *Radiother Oncol* 2014; **111**: 348–53. doi: 10.1016/j.radonc.2014.02.017
4. Pak K, Cheon GJ, Nam HY, Kim SJ, Kang KW, Chung JK, et al. Prognostic value of

metabolic tumor volume and total lesion glycolysis in head and neck cancer: a systematic review and meta-analysis. *J Nucl Med* 2014; **55**: 884–90. doi: 10.2967/jnumed.113.133801

5. Min M, Lin P, Lee MT, Shon IH, Lin M, Forstner D, et al. Prognostic role of metabolic parameters of 18F-FDG PET-CT scan performed during radiation therapy in locally advanced head and neck squamous cell carcinoma. *Eur J Nucl Med Mol Imaging* 2015; **42**: 1984–94. doi: 10.1007/s00259-015-3104-8
6. Chawla S, Kim S, Wang S, Poptani H. Diffusion-weighted imaging in head and neck cancers. *Future Oncol* 2009; **5**: 959–75. doi: 10.2217/fon.09.77
7. Baer AH, Hoff BA, Srinivasan A, Galbán CJ, Mukherji SK. Feasibility analysis of the parametric response map as an early predictor of treatment efficacy in head and neck cancer. *AJNR Am J Neuroradiol* 2015; **36**: 757–62. doi: 10.3174/ajnr.A4296
8. Chen Y, Liu X, Zheng D, Xu L, Hong L, Xu Y, et al. Diffusion-weighted magnetic resonance imaging for early response assessment of chemoradiotherapy in patients with nasopharyngeal carcinoma. *Magn Reson Imaging* 2014; **32**: 630–7. doi: 10.1016/j.mri.2014.02.009
9. Holdsworth SJ, Yeom K, Skare S, Gentles AJ, Barnes PD, Bammer R. Clinical application of readout-segmented- echo-planar imaging for diffusion-weighted imaging in pediatric brain. *AJNR Am J Neuroradiol* 2011; **32**: 1274–9. doi: 10.3174/ajnr.A2481
10. Bogner W, Pinker-Domenig K, Bickel H, Chmelik M, Weber M, Helbich TH, et al. Readout-segmented echo-planar imaging improves the diagnostic performance of diffusion-weighted MR breast examinations at 3.0 T. *Radiology* 2012; **263**: 64–76. doi: 10.1148/radiol.12111494
11. Porter DA, Heidemann RM. High resolution diffusion-weighted imaging using readout-segmented echo-planar imaging, parallel imaging and a two-dimensional navigator-based reacquisition. *Magn Reson Med* 2009; **62**: 468–75. doi: 10.1002/mrm.22024
12. Liney GP, Holloway L, Al Harthi TM, Sidhom M, Moses D, Juresic E, et al. Quantitative evaluation of diffusion-weighted imaging techniques for the purposes of radiotherapy planning in the prostate. *Br J Radiol* 2015; **88**: 20150034. doi: 10.1259/bjr.20150034
13. Horsman MR, Mortensen LS, Petersen JB, Busk M, Overgaard J. Imaging hypoxia to improve radiotherapy outcome. *Nat Rev Clin Oncol* 2012; **9**: 674–87. doi: 10.1038/nrclinonc.2012.171
14. Alonzi R, Hoskin P. Functional imaging in clinical oncology: magnetic resonance imaging- and computerised tomography-based techniques. *Clin Oncol (R Coll Radiol)* 2006; **18**: 555–70. doi: 10.1016/j.clon.2006.06.002
15. Rodrigues LM, Howe FA, Griffiths JR, Robinson SP. Tumor R2* is a prognostic indicator of acute radiotherapeutic response in rodent tumors. *J Magn Reson Imaging* 2004; **19**: 482–8. doi: 10.1002/jmri.20024
16. Baudelet C, Gallez B. How does blood oxygen level-dependent (BOLD) contrast correlate with oxygen partial pressure (pO2) inside tumors? *Magn Reson Med* 2002; **48**: 980–86. doi: 10.1002/mrm.10318
17. Chopra S, Foltz WD, Milosevic MF, Toi A, Bristow RG, Ménard C, et al. Comparing oxygen-sensitive MRI (BOLD R2*) with oxygen electrode measurements: a pilot study in men with prostate cancer. *Int J Radiat Biol* 2009; **85**: 805–13. doi: 10.1080/09553000903043059
18. Li XS, Fan HX, Fang H, Song YL, Zhou CW. Value of R2* obtained from T2*-weighted imaging in predicting the prognosis of advanced cervical squamous carcinoma treated with concurrent chemoradiotherapy. *J Magn Reson Imaging* 2015; **42**: 681–8. doi: 10.1002/jmri.24837
19. Schindelin J, Arganda-Carreras I, Frise E, Kaynig V, Longair M, Pietzsch T, et al. Fiji: an open-source platform for biological-image analysis. *Nat Methods* 2012; **9**: 676–82. doi: 10.1038/nmeth.2019
20. Harris AL. Hypoxia–a key regulatory factor in tumour growth. *Nat Rev Cancer* 2002; **2**: 38–47. doi: 10.1038/nrc704
21. Choi SH, Paeng JC, Sohn CH, Pagsisihan JR, Kim YJ, Kim KG, et al. Correlation of 18F-FDG uptake with apparent diffusion coefficient ratio measured on standard and high *b* value diffusion MRI in head and neck cancer. *J Nucl Med* 2011; **52**: 1056–62. doi: 10.2967/jnumed.111.089334
22. Schouten CS, de Bree R, van der Putten L, Noij DP, Hoekstra OS, Comans EF, et al. Diffusion-weighted EPI- and HASTE-MRI and 18F-FDG-PET-CT early during chemoradiotherapy in advanced head and neck cancer. *Quant Imaging Med Surg* 2014; **4**: 239–50. doi: 10.3978/j.issn.2223-4292.2014.07.15
23. Fruehwald-Pallamar J, Czerny C, Mayerhoefer ME, Halpern BS, Eder-Czembirek C, Brunner M, et al. Functional imaging in head and neck squamous cell carcinoma: correlation of PET/CT and diffusion-weighted imaging at 3 Tesla. *Eur J Nucl Med Mol Imaging* 2011; **38**: 1009–19. doi: 10.1007/s00259-010-1718-4